Journal of Power Sources 182 (2008) 160–167

Contents lists available at ScienceDirect

Journal of Power Sources

journal homepage: www.elsevier.com/locate/jpowsour

An innovative configuration of a Pd-based membrane reactor for the production of pure hydrogen
Experimental analysis of water gas shift

G. Barbieri[a,*], A. Brunetti[a,b], G. Tricoli[b], E. Drioli[a,b]

[a] National Research Council-Institute for Membrane Technology (ITM-CNR), Via Pietro BUCCI, c/o The University of Calabria, cubo 17C, 87030 Rende CS, Italy
[b] The University of Calabria, Department of Chemical Engineering and Materials, cubo 44A, Via Pietro BUCCI, 87030 Rende CS, Italy

ARTICLE INFO

Article history:
Received 23 January 2008
Received in revised form 19 March 2008
Accepted 20 March 2008
Available online 11 April 2008

Keywords:
Pure hydrogen production
Innovative membrane reactor
Water gas shift reaction
Volume index

ABSTRACT

Pure hydrogen production is of fundamental interest for its use as feed of proton exchange membrane fuel cells. In this work an innovative configuration for a membrane reactor (MR) was proposed: the membrane is located only in the second part of the catalytic bed. This configuration is of particular importance in all the reactions characterized by low kinetics such as, e.g., water gas shift (WGS). Permeation of hydrogen, in the desired direction, takes place when its partial pressure on the reaction side exceeds that on the permeate side. In an MR where the membrane starts at the reactor entrance there is a part of membrane area giving back permeation to the reaction side. The length used in a bad way depends on the kinetics: for fast kinetics reactions (e.g., methane steam reforming) it is very short but is significantly higher for reactions characterized by low kinetics (e.g., WGS). The innovative configuration proposed allows a good exploitation of the whole membrane area for the permeation.

This innovative Pd-alloy (60 μm thick) MR was used to analyse the WGS reaction at 280–320 °C, up to 600 kPa, GHSV ranging from 2000 h^{-1} to 4500 h^{-1}.

A significant reduction of the reaction volume required to achieve the same CO conversion was shown by the novel configuration of the MR with respect to the "typical" one used up to now.

1. Introduction

In the last few decades a great deal of attention has been attracted to the use of hydrogen as an energetic carrier to be employed for clean energy production by means of new technologies, such as polymer electrolyte fuel cells (PEMFCs). The new application of H_2 as feed in fuel cells for mobile power sources requires in the anode inlet gas a CO concentration lower than 10–20 ppm [1]. Otherwise, the anode is poisoned and the cell efficiency suddenly drops. Hence, if the H_2 is produced from hydrocarbon or alcohol reforming, purification is required in order to reduce the CO level to cell requirements. So far, the most technologically feasible purification train consists of a water gas shift (WGS) converter and a subsequent step of remaining CO elimination [2].

$$CO + H_2O = CO_2 + H_2, \quad \Delta H^{\circ}_{298K} = -41\ kJ\ mol^{-1}$$

WGS reaction is employed in industrial processes of H_2 production from liquid and gaseous hydrocarbons. The role of this reaction is to increase H_2 yield and decrease the CO concentration, which is, moreover, a poison for some catalysts used in downstream processing, as in ammonia synthesis or oil dehydrogenation. WGS reaction is traditionally carried out in two fixed bed adiabatic reactors, connected in series with a cooler between them. The first reactor operates at temperatures ranging from 300 °C to 500 °C and employs an Fe–Cr-based catalyst. The second reactor uses a CuO–ZnO-based catalyst and operates at lower temperatures (180–300 °C) in order to displace the equilibrium, since WGS reaction is exothermic. Recently, a renewed interest in the study of this reaction has arisen owing to H_2 application to fuel cells. Several works on different catalysts more active than the traditional ones, which can be used for H_2 production in fuel cell application, have been published. In the past, some authors [3] proposed the doping of CuO–ZnO-based catalysts. However, in the last few years, the majority of them have preferred the use of supported noble metals like ceria [4] instead of traditional catalysts. These new catalysts,

Abbreviations: GHSV, gas hourly space velocity (h−1); MR, membrane reactor; "innovative" MR, membrane reactor configuration proposed in this paper; "typical" MR, typical configuration of membrane reactor published in the open literature; MREC, MR equilibrium conversion; RI, recovery index; TR, traditional reactor; TREC, TRequilibrium conversion; VI, volume index; WGS, water gas shift.

* Corresponding author. Tel.: +39 0984 492029; fax: +39 0984 402103.
E-mail address: g.barbieri@itm.cnr.it (G. Barbieri).

0378-7753/$ – see front matter © 2008 Published by Elsevier B.V.
doi:10.1016/j.jpowsour.2008.03.086

Nomenclature

E	activation energy (J mol^{-1})
F	molar flow rate (mol s^{-1})
J	permeating flux (mol m^{-2} s^{-1})
P	pressure (Pa)
T	temperature (°C)
V	reaction volume (m^3)

Superscripts

Feed	membrane module inlet stream referred to
Permeate	membrane module outlet stream as permeate referred to
Retentate	membrane module outlet stream as retentate referred to

Acronyms

GHSV	gas hourly space velocity (h^{-1})
MR	membrane reactor
"innovative" MR	membrane reactor configuration proposed in this paper
"typical" MR	typical configuration of membrane reactor published in the open literature
MREC	MR equilibrium conversion
RI	recovery index
TR	traditional reactor
TREC	TR equilibrium conversion
VI	volume index
WGS	water gas shift

showing a higher activity with respect to the traditional ones, allow an operating range of 250–350 °C with good results given on a traditional reactor (TR) [5]. A promising approach for WGS reaction is the use of membrane reactors (MRs), combining the reaction and H_2 separation by means of a selective membrane.

WGS reaction is exothermic and characterized by no variation in the number of moles. Thus, CO equilibrium conversion is favoured by a low temperature and is independent of the reaction pressure in a TR. On the contrary, in an MR the reaction pressure has a positive effect on the equilibrium conversion of WGS reaction although it is characterized by no variation of mole number. In fact, a high pressure on the reaction side facilitates permeation and therefore, pushes the reaction towards further product formation [6–8]. The use of an MR, thus, allows a higher conversion to be reached also at a higher temperature where the thermodynamic conversion is low, acting positively on the kinetics. As a consequence, the catalyst amount necessary for a given conversion can be significantly reduced. For instance using a Pd-alloy MR, working at 280 °C and 1000 kPa, the catalyst volume necessary to reach 90% of the equilibrium conversion reduces to 1/4 of that of a TR [7].

In the past, Pd-alloy membranes were already successfully used for hydrogen production/separation also for the WGS step because of the infinite H_2 selectivity which allows a pure H_2 stream, not requiring further separations [9–11].

In the open literature, many studies were on the MRs with palladium membranes [12,13]. Seok and Hwang [14] evaluated the performance of the WGS reaction by using Vycor glass coated with ruthenium(III) chloride trihydrate. The reaction was carried out under various operating temperatures, pressures and feed compositions. The highest CO conversion obtained was 85% (equilibrium value 99.9%) at relatively low temperature (170 °C) and a sweep factor equal to 10, which means a sweep flow rate five times higher than the feed one. Complete conversion (100%) was obtained by Kikuchi et al. [8] and Uemiya et al. [11] at 400 °C using a tube in tube MR, in which the inner tube consisted of a thin palladium film, also by using a sweep factor equal to 10. Tosti et al. [15] added silver to palladium to decrease membrane embrittlement and to increase the hydrogen permeability. They developed a WGS MR with a Pd–Ag film (50 μm thick) covering the external side of a ceramic porous tube and achieved reaction conversions close to 100% (well above the equilibrium value of 80%) at 325–330 °C, owing to a high sweep gas flow rate.

However, the majority of these studies proposed the use of sweep gas to promote the H_2 permeation, while only a small part combines the use a low feed pressure at the sweep gas for improving the permeation. An important role should be assigned to this variable, used instead of sweep gas, which promotes the H_2 permeation allowing, at the mean time, a pure H_2 stream to be obtained.

A fundamental aspect in the Pd-alloy MR use is the good exploitation of whole the available membrane area that improves the global MR performance, assuring a higher CO conversion and also more H_2 recovered in the permeate side. However, the hydrogen permeated depends not only on the membrane properties such as the permeance, but it is also a linear function of the driving force, which in the case of Pd–Ag MRs generally is given by the difference of the square root of the H_2 partial pressure on both side of the membrane (*Sieverts*' law). As studied in our previous work [16], in the first part of an MR the H_2 partial pressure starts from zero since it is not present in the feed stream, but it is only produced by reaction (Fig. 1-left side). As a consequence, in this reactor section the H_2 partial pressure is very low, implying back permeation. This means a bad utilization of the first part of the membrane area and thus, a worsening of the MR performance with lower H_2 recovery and lower CO conversion with respect to the case in which the whole selective surface is useful used. To avoid this problem, in this work a different MR configuration is proposed, improving the idea of an MR in series to a TR already introduced in a previous work [17]. The two reactors of [17] were combined in one unit: the innovative MR here proposed has the Pd-based membrane located only in the second part of the catalytic bed. The first section is characterized only by chemical reaction whereas in the second part also the permeation through the membrane takes place: the reaction starts at the reactor entrance producing H_2 and its permeation starts only where its partial pressure is high.

Fig. 1 shows the dimensionless partial pressure profiles for the MR in "typical" (left side) and innovative (right side) configurations: the whole membrane area is exploited with the new solution and higher H_2 recovery and thus, CO conversion can be achieved.

2. Materials and methods

2.1. Experimental apparatus

In an MR, the permeation takes place in the desired direction only when there is a positive driving force, i.e., the specie partial pressure on the reaction side is higher than that on the permeate side. This condition is not always present along the whole MR length, in particular when only the reactants are fed and the permeation is desired for a product. This is the case of reactions for hydrogen production or its upgrading into Pd-alloy MRs.

If only reactants are fed, no hydrogen is present at the MR entrance; therefore, no permeation is possible in the desired direction, but permeation, which happening in any case, takes place in the undesired direction: from the permeation to the reaction side. This happens up to the MR length where the hydrogen partial pressure on the reaction and permeation sides are equal. After this point the permeation is realized in the desired direction.

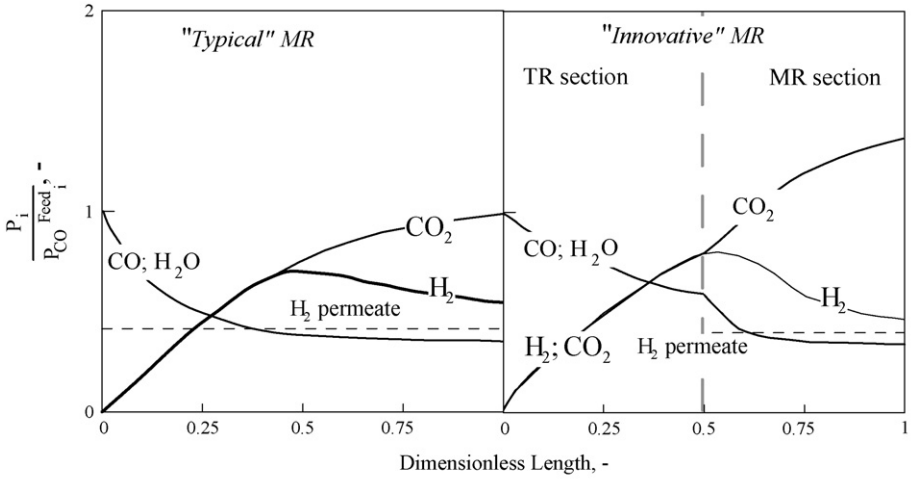

Fig. 1. Dimensionless partial pressure profiles as a function of membrane length for a "typical" and an "innovative" MR configuration.

The location of the "breakthrough" along the reactor length depends on the kinetics. For instance, in the methane steam reforming, characterized by a high kinetics, the undesired permeation is confined to a very small reactor length. In WGS reaction (particularly at a low temperature) the kinetics is slow and the "breakthrough" is at a significant reactor length.

Barbieri and Bernardo [17] proposed a solution where a "typical" MR operates on the downstream of a TR. In the first reactor, CO and H_2O were partially converted in H_2 and CO_2. The feed of the second reactor (the MR) contains also hydrogen thus, the permeation starts at the MR entrance.

The novel design proposed in this paper (Fig. 2) couples both reactors in one unit. It consists of a catalytic bed ("TR" section) followed by a "typical" MR where a Pd-based membrane is deep in the second part of the catalytic bed (Fig. 2). Therefore, only reaction takes place in the first section and in the second part also permeation is operated. It couples the advantage to feed the reactants and to overcome the undesired back permeation of hydrogen.

H_2 partial pressure profile (reaction side) increases in the TR section after which, in the MR part, decreases due to the permeation which prevails on the production by reaction. On the other membrane side, the pressure drop (even though it can be very small as in the present case) imposes the trend. In the configuration proposed in this work (cocurrent flows) both (retentate and permeate) H_2 profiles have the same trend (in the MR section) due to the permeation and pressure drop (respectively). Therefore, the permeation driving force remains always positive (Fig. 1, right side).

In the case of countercurrent flows, the H_2 profile on the permeate side will be opposite to that on the reaction side with a lower difference at the reactor exit and higher value at the membrane exit (central part of the reactor). This produces an average driving force for permeation lower than in the cocurrent case. Of course, the difference in the performance of the innovative MR will be visible depending on the fullness of the pressure drop. In the present case, with very low-pressure drop the two configurations are equivalent.

A different situation is presented when a reformate stream is fed to a WGS MR due to the high content of hydrogen in the fed stream. In this case a "typical" MR shows its peculiar characteristic in improved performance with respect to a TR.

The "innovative" MR (Fig. 2) was realized assembling a tubular blind Pd–Ag membrane in a stainless steel shell, filling the tubular (TR section) and annular ("typical" MR part) volumes with CuO/CeO_2 catalyst. The innovative MR characteristics are resumed in Table 1.

A scheme of the experimental apparatus used in permeation and reaction tests is shown in Fig. 3. The MR was placed in a temperature controlled electric furnace (with PID control). Mass flow controllers (Brooks Instrument 5850S) were used for feeding all the inlet gaseous streams, while an HPLC pump (Dionex P680A) was used to feed the water. A heating coil line was put into the furnace to vaporize the water. The flow rates of the outlet streams were measured by means of bubble soap flow meters. The chemical analyses on the retentate and permeate streams were performed by means of a gas chromatograph (Agilent 6890N) with two parallel analytical lines. Each line is equipped with two columns: an HP-Plot-5A (for separating permanent gases such as H_2, N_2 and CO) and an HP-Poraplot-Q (for other species) and a TCD.

Pd-alloy dense membranes are generally utilised in a temperature range where the diffusion in the metal bulk is the rate determining step. *Sieverts*' law (Eq. (1)) is used worldwide for the mathematical description of H_2 permeating flux in these membranes. The hydrogen flux is a linear function of the driving force, which, when the diffusion through the bulk is the rate determining step, such as in the present case, is given by the difference of the

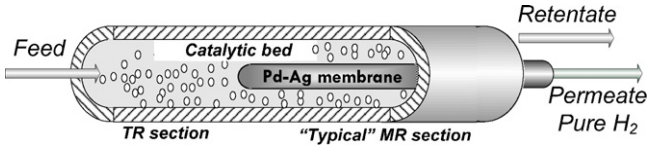

Fig. 2. Configuration of the "innovative" MR.

Table 1
Innovative MR characteristics

TR section	
Length	8 cm
Catalyst amount	1.7 g
MR section	
Length	9.5 cm
Membrane type	Pd–Ag: commercial (Johnsonn–Matthey) self-supported
Membrane thickness	60 μm
Superficial area	2 cm^2
Catalyst amount	1.7 g

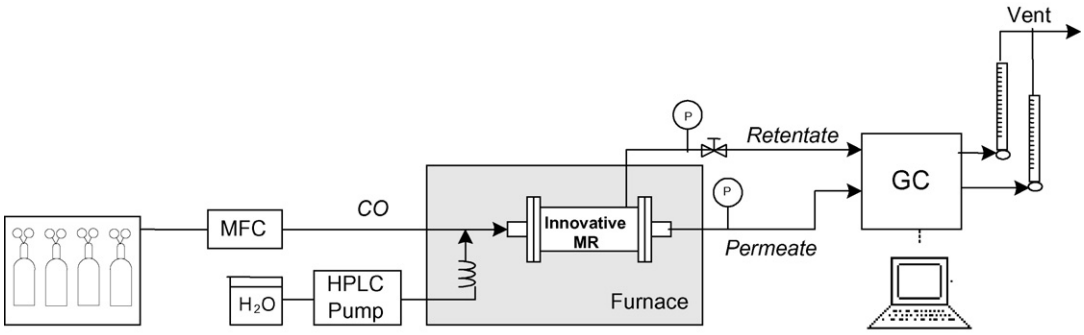

Fig. 3. Scheme of the experimental laboratory-scale plant. MFC: mass flow controller; GC: gas chromatograph.

square root of the H_2 partial pressure on both membrane sides (Eq. (2)).

$$J_{H_2}^{\text{Permeating}}\ (\text{mol m}^{-2}\,\text{s}^{-1}) = \text{Permeance}_{H_2}^{0}\, e^{-E/RT}\, \Delta\sqrt{P_{H_2}} \quad (1)$$

$$\Delta\sqrt{P_{H_2}}\ (\text{Pa}^{0.5}) = \Delta P_{H_2}^{\text{Sieverts}} = \sqrt{P_{H_2}^{\text{reaction side}}} - \sqrt{P_{H_2}^{\text{permeation side}}} \quad (2)$$

CO conversion of a TR and MR was calculated using Eq. (3), including the CO and CO_2 present in the outlet streams.

$$\text{CO conversion} = \frac{1}{2}\left\{\left(\frac{F_{CO_2}^{OUT}}{F_{CO}^{Feed}}\right) + \left(1 - \frac{F_{CO}^{OUT}}{F_{CO}^{Feed}}\right)\right\} \quad (3)$$

The conversion is calculated as the arithmetic average value between that calculated from the CO_2 yield (lower limit) and that corresponding to the CO present in the outlet stream. The difference of the two values is the carbon balance.

The upper limit of a chemical reaction is given by the thermodynamic equilibrium conversion. While that of a TR (TREC) is a widely consolidated concept, the equilibrium of an MR is a relatively new concept [6]. The permeation equilibrium has to be reached in an MR in addition to the reaction equilibrium typical of a TR.

Therefore, the MR equilibrium conversion (MREC) is a function of the thermodynamic variables and initial composition on both sides of the Pd-alloy membranes.

$$\begin{aligned}\text{MREC} &= \text{MR equilibrium conversion}\\ &= f\left(Kp, T^{\text{Reaction}}, P^{\text{Reaction}}, Y_i^{\text{Feed}}, T^{\text{Permeation}},\right.\\ &\quad \left. P^{\text{Permeation}}, \frac{F^{\text{Feed}}}{F^{\text{Sweep}}}, Y_i^{\text{Sweep}}\right),\end{aligned} \quad (4)$$

MREC is independent of the membrane permeation properties influencing the time-dependent variables (e.g., the residence time MR) necessary to reach equilibrium, but the final value reached depends on the extractive capacity of the system. The MREC is the maximum conversion achievable with the MR, for set operating conditions.

A fundamental variable to consider in the study of the MR performance for producing H_2 is the recovery capability of MR, the recovery index (Eq. (5)), defined as [7]:

$$H_2 \text{ recovery index } (RI_{H_2}) = \frac{F_{H_2}^{\text{Permeate}}}{F_{H_2}^{\text{Permeate}} + F_{H_2}^{\text{Retentate}}} \quad (5)$$

Estimated from the reactor outlet streams, it represents the H_2 fraction permeated through the membrane with respect to the total H_2 produced by reaction.

An important parameter in the design of new plants is the volume index (VI) (Eq. (6)) that comparing the MR reaction volume with that of a TR necessary to achieve a set conversion [16].

$$\text{Volume index (VI)} = \left.\frac{V_{\text{Reaction}}^{\text{MR}}}{V_{\text{Reaction}}^{\text{TR}}}\right|_{\text{Set CO Conversion}} \quad (6)$$

In this work, the VI was calculated for the innovative MR, in order to evaluate the gain in term of reduction of reaction volume and catalyst with respect to a TR.

For the evaluation of these indexes, an experimental work was carried out. The permeating flux was measured feeding pure H_2 before the reaction, for evaluating the permeation membrane properties (flux and permeance) as a function of the temperature.

Reaction tests were carried out on the novel system at the operating conditions reported in Table 2.

A commercial CuO/CeO_2-based catalyst (Engelhard) was packed in both (TR and "typical" MR) sections of the innovative MR.

An equimolecular H_2O/CO stream was used in the reaction experiments, on the basis of previous studies. No sweep gas was used during the tests because, as discussed in the introduction, one of the main aims of this work is the study of the feed pressure effect on the performance of the system in obtaining a pure hydrogen stream as permeate.

The GHSV for the "innovative" MR, was calculated by using the following equation:

$$\frac{1}{\text{GHSV}_{\text{Innovative MR}}} = \frac{1}{\text{GHSV}_{\text{TR}}} + \frac{1}{\text{GHSV}_{\text{MR}}} \quad \text{h} \quad (7)$$

3. Results and discussion

3.1. Permeation tests

A linear dependence of the H_2 flux as a function of the driving force (Eq. (1)) was observed at all the temperatures investigated (Fig. 4), being the difference among experimental results and linear regression through the origin lower than 3% and the error bars are practically drawn inside the symbol itself. Therefore, the permeation measurements confirm that hydrogen flux follows *Sieverts*' law, thus, a constant permeance value can be assumed for each

Table 2
Reaction tests operating conditions

Temperature	280–320 °C
Feed pressure	200–600 kPa
Permeate pressure	100 kPa
H_2O/CO feed molar ratio	1
GHSV	2170–10000 h^{-1}
No sweep	

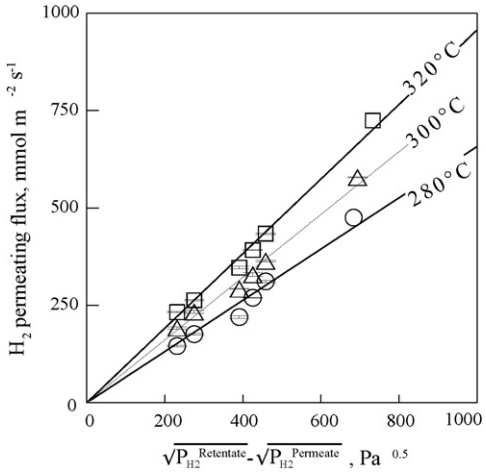

Fig. 4. Pd–Ag membrane permeation tests up to a feed pressure of 1000 kPa. Hydrogen permeating flux as a function of $\Delta\sqrt{P_{H_2}}$ (driving force of *Sieverts*' law) at different temperatures. Symbols: measured data; lines: linear regression through the axes origin.

Table 3
Arrhenius parameters

Feed stream	Frequency factor (mol m^{-2} s^{-1} Pa^{-1})	E (kJ mol^{-1})
Pure H_2	0.12 (±0.05)	2.9 (±0.2)
During WGS reaction		
2070 h^{-1}	168 (±51)	7.3 (±0.3)
3180 h^{-1}	700 (±300) 10^6	16.5 (±4.7)
4550 h^{-1}	800 (±110) 10^6	16.9 (±0.21)

temperature. Fig. 5 shows H_2 permeance (Arrhenius plot) measured feeding a pure H_2 stream or during WGS reaction. H_2 permeance increases with the temperature at any GHSV. CO average concentration in the MR depends, at the same operating conditions, on the GHSV: a higher GHSV value implies that the unconverted CO is higher too. The presence of CO was demonstrated [18] having a reducing effect on H_2 permeation. The present results agree with the prevision of the new model equation proposed by [18] even if they used a temperature of 374 °C in their experiments. Table 3 reports the parameters of the Arrhenius plot for hydrogen permeance calculated by experimental results of Fig. 5.

The H_2 permeance during the reaction showed a reduction owing to CO presence that inhibits the H_2 permeation. This H_2 permeance reduction can be estimated by using the following equation:

$$H_2 \text{ permeance reduction} = \alpha = 1 - \frac{\text{Permeance}_{H_2}^{\text{During reaction}}}{\text{Permeance}_{H_2}^{\text{Permeation tests}}} \quad (8)$$

In particular, for a set temperature, the H_2 permeance reduction is higher at a higher space velocity (Fig. 5). In this case, CO conversion being lower (as will be shown in the section related to reaction tests), CO partial pressure in the retentate side is higher, with consequent higher inhibition effects. These are less evident at higher temperature because the adsorption phenomenon decreases significantly with the temperature.

3.2. Reaction tests

WGS is a reaction taking place without mole number variation, therefore in a TR no effect on the reaction can be shown by the feed pressure variation from the thermodynamics point of view. On the contrary, in an MR, the feed pressure promotes the selective removal of H_2 from reaction volume and, thus, shifts the equilibrium limit [7] towards a higher CO conversion.

Fig. 6 shows CO conversion as a function of the feed pressure at 300 °C for different GHSVs. A monotonic increasing trend of CO conversion with the feed pressure is shown at all the GHSVs. In particular, at 2070 h^{-1}, typical condition in industrial applications, CO conversion is always higher than TREC and is close to MREC values at all the feed pressures investigated. This advantage is reduced at a higher GHSV (3180 h^{-1}) where TREC is exceeded for feed pressures higher than 400 kPa. A low GHSV means high space-time, thus, higher contact time among reactants and catalyst that allows higher CO conversion, at the same operating conditions. Increasing the GHSV, the space-time is lower therefore, CO conversion decreases. However, good CO conversion is obtained also at a higher GHSV and it exceeds also the conversions achieved in a TR, increasing the feed pressure. H_2 removal from the reaction volume, in fact, acts positively on the conversion partially compensating the reduction of contact time among reactants and catalyst.

Fig. 7 shows the CO conversion as a function of the temperature for the innovative MR and TR at 600 kPa. The curves show a

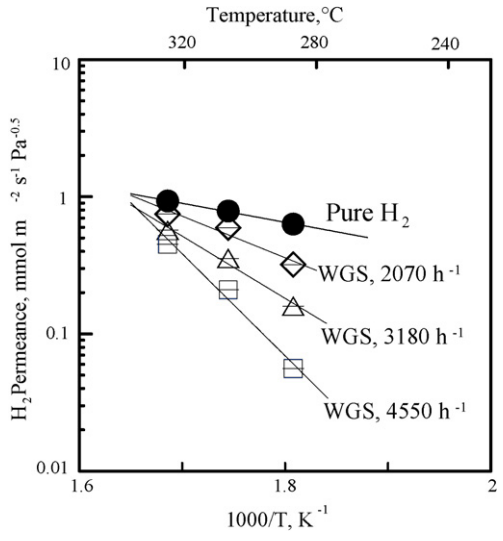

Fig. 5. H_2 permeance as a function of the temperature for pure H_2 feeding stream and during WGS reaction.

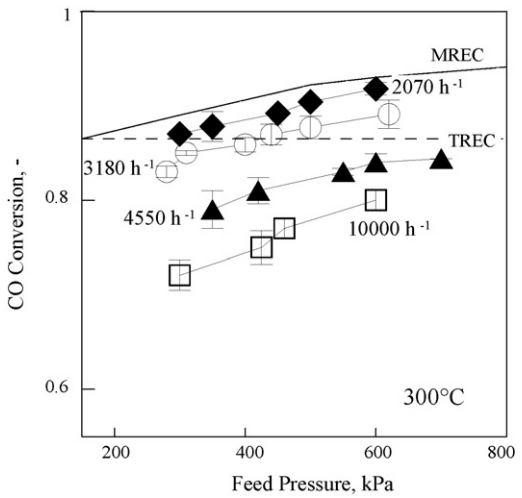

Fig. 6. CO conversion as a function of feed pressure at different GHSVs.

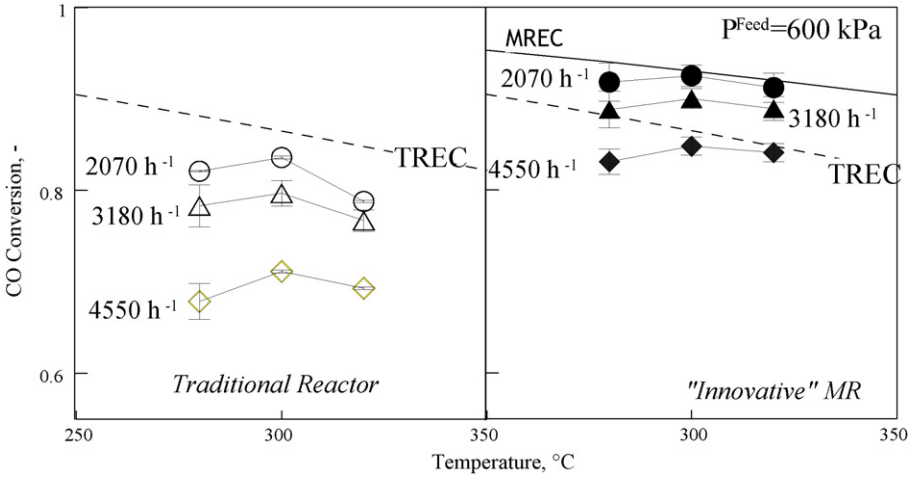

Fig. 7. CO conversion as a function of temperature at three GHSVs.

maximum at ca. 300 °C, at all the GHSVs values. At a low temperature, the kinetics and permeation are slow, even if the reaction is favoured by a thermodynamic point of view. A high temperature favours the kinetics and, specifically, the permeation; therefore, the more H_2 is removed from the reaction volume, the more the CO conversion improves. However, WGS being an exothermic reaction, increasing the temperature the thermodynamic limitations become more relevant reducing the equilibrium conversion and the measured conversion closely follows this trend.

MR CO conversion always significantly higher than the TR one exceeds the TREC for some operating conditions. At 2070 h^{-1}, CO conversion is completely closed to the MREC, always exceeding TREC, achieving the highest CO conversion of ca. 93% at 280 °C. Also at 3180 h^{-1} and 600 kPa the CO conversion is always higher than TREC, reaching 90% at 300 °C. At a higher GHSV, the MR CO conversion reduces under the TREC, becoming the same as TR at a lower temperature. This is owing to the lowest contact time among reactant and catalyst that depletes the CO conversion, in addition the reduced permeation owing to the low temperature is added. Even if the CO conversion is lower than TREC, it is much higher than TR in the same operating conditions.

An important parameter in the analysis of the MR is the recovery index, useful to give an evaluation of the extractive capacity of the system, the ratio being between the H_2 amount recovered as permeate with respect to the total H_2 produced by the reaction (Eq. (5)).

The RI as a function of the driving force of the process (Eq. (1)) is reported in Fig. 8 at three temperatures. The H_2 recovered in the permeate stream increases linearly with the driving force at all the temperatures and GHSVs considered. At a low GHSV the H_2 recovered is high owing to the higher CO conversion achieved, therefore, the best recovery (ca. 75%) is obtained at 2070 h^{-1} for all the temperatures investigated. Furthermore, at the same GHSV, the RI increases with the temperature, because of its positive effect on permeation.

The best results are obtained at the highest temperature (320 °C) operating at the lowest GHSV (2070 h^{-1}) where ca. 75% of the H_2 produced is recovered in the permeate side (Fig. 9). Even if at a relatively high temperature the CO conversion is lower owing to the thermodynamics, however, the H_2 permeation is strongly favoured, thus, more H_2 is recovered as pure stream in the permeate side.

This behaviour is more evident at high feed pressure that, acting also positively on the permeation, allows more H_2 to be recovered on the permeate side (Fig. 9).

A relationship among the hydrogen recovery index and the operating conditions is highly desired. The peculiarities of the membrane performance combined with those of the reaction ones have to be taken into consideration to find this relationship. The membrane performance during reaction can be related to its permeance and specifically also to its reduction due to the CO presence that obstacles the H_2 flux. CO concentration is a function of the progress of the reaction. The reaction affects the hydrogen

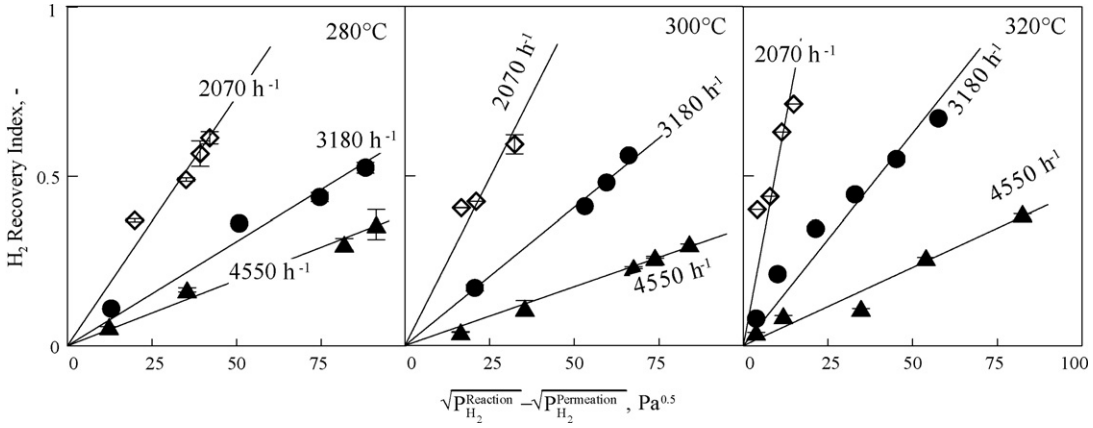

Fig. 8. Recovery index as a function of $\Delta\sqrt{P_{H_2}}$ at three GHSVs and three temperatures.

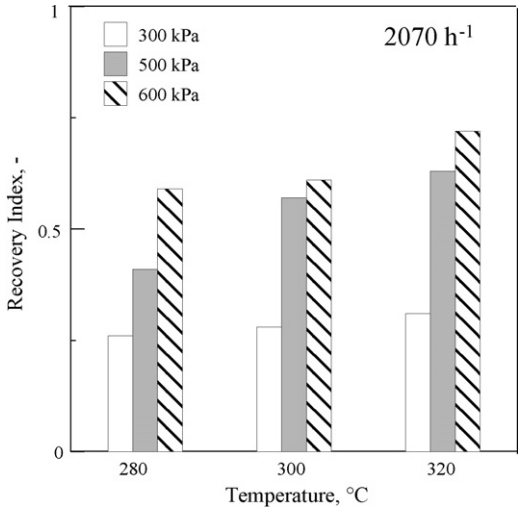

Fig. 9. Recovery index as a function of temperature at three feed pressures.

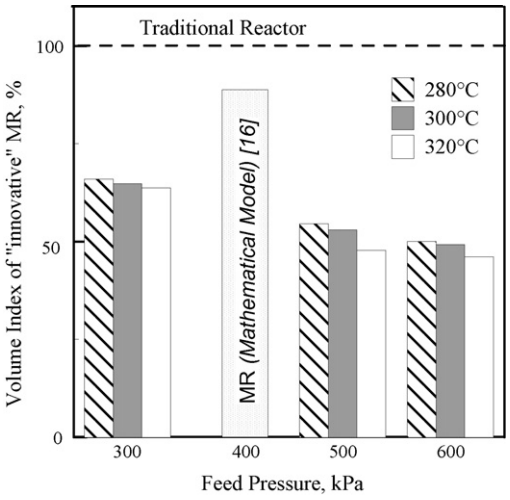

Fig. 11. Volume index evaluated by experimental data as a function of feed pressure at three temperatures.

production and hence its partial pressure. GHSV can be considered to indicate the reaction performance or better (specifically) the hydrogen production. Therefore, the following Eq. (9) was obtained to represent the RI lines at all the GHSVs.

$$\mathrm{RI} = k\frac{\mathrm{GHSV}_0}{\mathrm{GHSV}}\frac{1}{\alpha}\Delta\sqrt{P_{\mathrm{H_2}}} \quad (9)$$

It considers any increases of GHSV with respect to the reference values GHSV_0 and the permeance reduction by means of Eq. (8).

Fig. 10 shows this correlation for the three temperatures of Fig. 9. There is a very good agreement between the experimental points and the regression lines through the origin. Therefore, Eq. (9) well represents the H_2 RI as function of the GHSV, feed pressure, etc. at any investigated temperature.

The proportional factor, k, has to be evaluated at each temperature. It does not have a regular dependence on the temperature because the reaction approaches the chemical equilibrium at the highest temperature.

As an index of the reduced size of the system, the VI was analysed considering the innovative MR configuration, for evaluating the gain in term of reaction volume with respect to a simple TR (Fig. 11). VI is a decreasing function of the feed pressure, at a set temperature. The reaction volume of MR is around 50% of that of a TR (VI = 0.5), to achieve a final conversion of ~80% (corresponding to 90% of the TREC), working at a feed pressure higher than 300 kPa. Furthermore, at a temperature higher than 280 °C, the VI is still reduced. A high feed pressure and a high temperature, in fact, implying that more H_2 permeates through the membrane, shifting

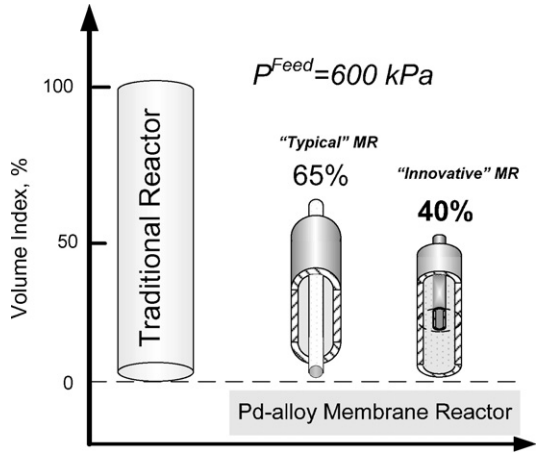

Fig. 12. Comparison of the volume index of "typical" MR and innovative MR configurations.

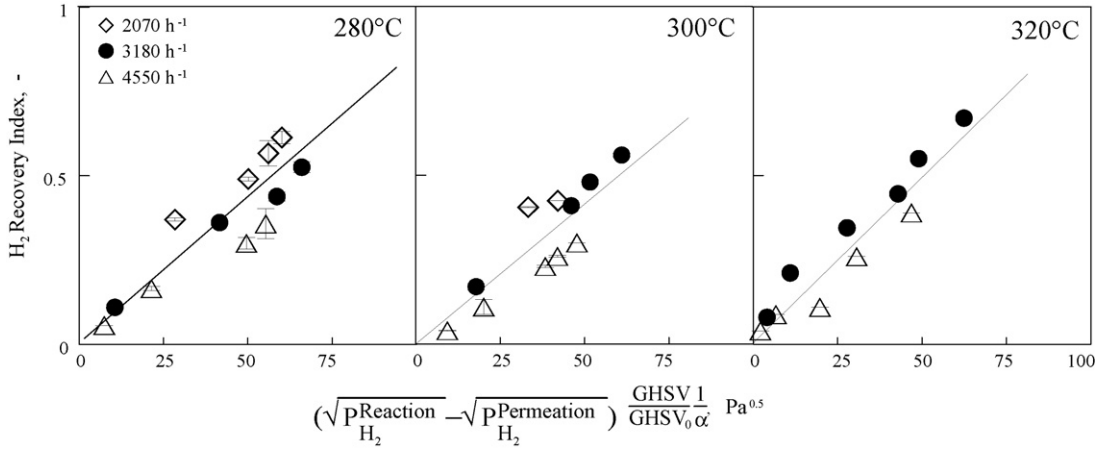

Fig. 10. Recovery Index as a function of $\Delta\sqrt{P_{\mathrm{H_2}}}$ at three GHSVs and three temperatures.

the reaction towards further CO conversion, requiring less catalyst amount, for achieving a set conversion. The same figure shows a comparison with some of our previous results obtained by simulating a "typical" MR in the same operating conditions [16]. A VI of ca. 85% was calculated at 400 kPa and 280 °C for the MR; the innovative MR shows a VI equal to ca 65%, already at 300 kPa. Furthermore, at 600 kPa it shows a VI of 40%, lower than that shown by simple MR (65%) at the same operating conditions (Fig. 12). This shows the clear gain in the use of the innovative solution that, allowing the problems related to the good exploitation of the membrane area to be overcame, shows further reaction volume reduction with respect to that achieved with the traditional MR.

4. Conclusion

The innovative MR configuration proposed in this work allows the exploitation of the whole Pd-based membrane surface. In fact, the membrane operates only in the second part of the catalytic bed where the hydrogen partial pressure is high enough to promote the permeation in the desired direction, from the reaction to permeate side. The first section of the catalytic bed works converting the reactants (the only species present in the feed stream) into hydrogen. This novel configuration is necessary, in particular, when no sweep gas is used (as in the present study). The partial pressure of hydrogen on the permeate side is equal to the total pressure and it is much higher than the partial pressure on the reaction side. Therefore, the presence of the membrane at the initial reaction stage (reactor entrance) gives a back permeation which has been overcame by the novel MR configuration proposed.

The performance of the novel MR was evaluated in term of CO conversion, H_2 recovery, lower reaction volume required, etc. for the water gas shift reaction, using a Pd–Ag membrane 60 micron, operating at 280–320 °C and up to 600 kPa. No sweep gas was used to promote the permeation but only the pressure difference between the two membrane sides. Therefore, pure H_2 was obtained as permeate stream.

Conversion is much higher than that of a TR operating in the same conditions and also significantly exceeds the equilibrium value of a TR (TREC). A conversion of 93% was measured at 300 °C and 600 kPa operating at 2000 h^{-1}; 70% of the H_2 produced by reaction was collected as pure permeate stream. recovery index (at each temperature) is a linear function of the permeation driving force, permeance in the actual condition and space velocity. It increases with the permeation driving force, H_2 permeance and conversion (owing to the higher H_2 production) but decreases with space velocity.

A significant reduction of the volume required to achieve the same CO conversion was shown by the novel MR configuration with respect to the "typical" one used up to now. In fact, the reaction volume (equivalent to the catalyst volume) required by the innovative MR is 40% (at 600 kPa and 280 °C) of that a TR instead of the 65% of the typical MR.

Acknowledgements

The Italian Ministry for Foreign Affairs, Direzione Generale per la Promozione e la Cooperazione Culturale, Rome (Italy) is gratefully acknowledged for co-funding this research. Johnsonn Matthey (UK) and Oleg M. Ilinitch (Engelhard, USA) are gratefully acknowledged for the membrane and catalysts supplied.

References

[1] F. Barbir, Solar Energy 78 (2005) 661–669.
[2] T.S. Yu, J.S. Dong, H.J. Jin, L.Y. Wang, J. Power Sources 163 (2006) 119–124.
[3] K. Klier, Ch. Young, J. Nunan, IEC Fund. 25 (1986) 36–42.
[4] Y. Li, Q. Fu, M.F. Stephanopoulos, Appl. Catal. B: Environ. 27 (2000) 179–191.
[5] P. Giunta, N. Amadeo, M. Laborde, J. Power Sources 156 (2006) 489–496.
[6] G. Barbieri, G. Marigliano, G. Perri, E. Drioli, Ind. Eng. Chem. Res. 40 (2001) 2017–2026.
[7] G. Barbieri, A. Brunetti, T. Granato, P. Bernardo, E. Drioli, Ind. Eng. Chem. Res. 44 (20) (2005) 7676–7683.
[8] E. Kikuchi, S. Uemiya, N. Sato, H. Inoue, H. Ando, T. Matsuda, Chem. Lett. (1989) 489–496.
[9] J. Shu, B.P.A. Grandjean, A. Van Neste, S. Kaliaguine, Can. J. Chem. Eng. 69 (1991) 1036–1048.
[10] F.A. Lewis, Palladium Hydrogen System, Academic Press, London, New York, 1967.
[11] S. Uemiya, N. Sato, H. Inoue, H. Ando, E. Kikuchi, Ind. Eng. Chem. Res. 30 (1991) 585–589.
[12] R. Dittmeyer, V. Hollein, K. Daub, J. Mol. Catal. A: Chem. 173 (2001) 135–184.
[13] S.N. Paglieri, J.D. Way, Sep. Purif. Methods 31 (2002) 1–169.
[14] D.R. Seok, S.T. Hwang, in: M. Misono, Y. Moro-oka, S. Kimura (Eds.), Future Opportunities in Catalytic and Separation Technology, Elsevier, Amsterdam, 1990, pp. 248–267.
[15] S. Tosti, A. Basile, G. Chiappetta, C. Rizzello, V. Violante, Chem. Eng. J. 93 (2003) 23–30.
[16] A. Brunetti, C. Caravella, G. Barbieri, E. Drioli, J. Membr. Sci. 306 (1–2) (2007) 329–340.
[17] G. Barbieri, P. Bernardo, Carbon Dioxide Capture for Storage in Deep Geologic Formations—Results from CO_2 Capture Project, vol. 1, Elsevier, 2004, pp. 385–408 (Chapter 2).
[18] G. Barbieri, F. Scura, F. Lentini, G. De Luca, E. Drioli, Sep. Purif. Technol. 61 (2007) 217–224.